

## 34.0 IN-SITU OBSERVATION OF PHASE AND TEXTURE EVOLUTION PRECEDING ABNORMAL GRAIN GROWTH IN NI-BASED AEROSPACE ALLOYS

Byron McArthur (Mines)  
 Faculty: Amy Clarke (Mines) and Kester Clarke (Mines)  
 Industrial Mentors: Kevin Severs (ATI)

This project initiated in Fall 2017 and is supported by CANFSA. The research performed during this project will serve as the basis for a Ph.D. thesis for Byron McArthur.

### 34.1 Project Overview and Industrial Relevance

Nickel-based superalloys are utilized extensively in the aerospace industry for their excellent high temperature strength, fatigue life, oxidation resistance and corrosion resistance. Turbine engine discs are flight critical components, and failure of these components risk loss of the entire plane. With the continuous push for more efficient commercial aviation, higher operating temperatures and pressures are desired. Complex Ni-based superalloys are being processed through novel methods to meet these stringent requirements.

The alloy utilized in the present study is RR1000, a  $\gamma$ - $\gamma'$  disk alloy with approximately 45% volume fraction of  $\gamma'$  at room temperature. Processing steps include alloyed powderization, hot isostatic pressing and extrusion at a 4.5:1 reduction ratio [34.1]. These steps produce a fully dense, recrystallized billet with  $\gamma$  grain size of 1-5  $\mu\text{m}$  diameter and a distribution of primary  $\gamma'$  (1-3  $\mu\text{m}$ ) and secondary  $\gamma'$  (20-50 nm). Two material conditions provided are shown in **Figure 34.1**, note the significant difference in fraction of primary  $\gamma'$ . Subsequent isothermal deformation processing of slices of material is performed near the  $\gamma'$  solvus temperature; secondary  $\gamma'$  is dissolved while primary  $\gamma'$  pins the  $\gamma$  grain boundaries and superplastic deformation keeps flow stresses low. Super-solvus heat treatment (SSHT) allows for  $\gamma$  growth to approximately 50  $\mu\text{m}$  for increased creep resistance during service [34.1]. Abnormal grain growth (AGG) has been shown to occur during the SSHT based upon processing parameters in the isothermal deformation ( $\epsilon$ ,  $\dot{\epsilon}$ , T) and SSHT heating rate. The AGG results in  $\gamma$  grains up to 3 mm that compromise mechanical performance and are difficult to detect via non-destructive testing (NDT). The objective of this project is to better understand the microstructural mechanisms that cause AGG in these materials through use of advanced, in-situ experimental techniques.

### 34.2 Previous Work

Prior research into AGG has been most successful in exploring the processing parameters required to produce AGG in an effort to prevent the phenomena from occurring in industrial components. Huron et al. [34.2] performed double cone isothermal compression testing on a similar alloy (René 88DT) and found a range of strain rates and deformation temperatures that produce AGG; increasing deformation temperature required higher strain rates to produce AGG. Parr et al. [34.3] did similar testing on RR1000 and found AGG conditions to occur at near- $\gamma'$ -solvus deformation temperatures, low strain rates, and low strains; similar to those explored in the present study. In-depth work performed by Payton [34.4] explored characterization techniques in an effort to understand the microstructural mechanism behind AGG; results indicated stored energy within the  $\gamma$  grains was a likely contribution to AGG, however combined contributions from  $\gamma'$  coherency changes and redistribution are important as well.

Work further exploring the AGG mechanisms has been performed by Charpagne et al. [34.5], and proposes that stored energy is the driving force for AGG, with static recrystallization of  $\gamma$  grains initiating the process. The recrystallization of the  $\gamma$  grains has been proposed by Charpagne to occur coherently off of primary  $\gamma'$ , proceeded by growth to consume neighboring  $\gamma$  grains containing stored energy; this mechanism has been termed 'heteroepitaxial recrystallization' (HERX). The coherency allows for a reduced energy barrier for recrystallization of the  $\gamma$ , theoretically occurring at lower temperatures. Interestingly, the  $\gamma$  grain boundaries appear to pass through large primary  $\gamma'$  with relatively low Zener pinning influence. Charpagne's work demonstrated continued growth of  $\gamma$  grains within critical regions until impingement upon each other limited growth, indicating nucleation limited events of grains that grow at the expense of unrecrystallized grains. The nucleation limited growth may be explained by inhomogenous distributions of stored energy that is a precursor to static recrystallization. Tu et al.'s work [34.6] supports this through strain mapping characterization techniques demonstrating significant grain-to-grain variations in plastic strain accumulation as well as changes in deformation mechanisms near the critical strain rates required for AGG. Based upon prior research, it

appears that stored energy, accumulated inhomogeneously during isothermal forging, creates the precursor requirements for AGG.

Prior work performed in this study focused on establishing the thermomechanical processing parameters for producing AGG in the experimental RR1000 materials. The main portion of this research so far has focused on the material with the starting condition shown in **Figure 34.1a**, containing a lower fraction of primary  $\gamma'$ , smaller secondary  $\gamma'$  and larger  $\gamma$  grains, as this material has shown instances of AGG during testing. Thermomechanical processing of the material with the starting condition shown in **Figure 34.1b** has not yet demonstrated instances of AGG. This is likely due to increased amounts of primary  $\gamma'$  influencing the deformation and recrystallization.

### 34.3 Recent Progress

#### 34.3.1 Thermomechanical Processing to Produce Abnormal Grain Growth

Isothermal compression of RR1000 specimens prepared via wire electron discharge machining was performed in a Gleeble® thermomechanical simulator. This allowed for control of deformation temperature, strain, and strain rate as well as providing load-displacement data. Post-deformation SSHT of the material utilized a TA Instruments quenching dilatometer to maintain precise temperature and heating rate control, as well as measure qualitative  $\gamma'$  dissolution and  $\gamma$  grain growth behavior through changes in length. The deformation temperature, strain rate, and strain utilized in the Gleeble® to produce AGG were 1110°C, 0.0008  $\epsilon/s$  and 0.16  $\epsilon$ , respectively. Utilizing the dilatometer, a low heating rate (0.12°C/s) up to the SSHT temperature promoted AGG occurrence.

Initial testing of Gleeble® specimens produced a significant axial thermal gradient that resulted in a gradient in microstructure and local strain accumulation. Changes in experimental setup and larger specimens allowed for isothermal forging under repeatable conditions, with reduced thermal gradients. Additionally, large specimens allowed for lower spatial gradients in strain, strain rate and temperature; increasing the region size for microstructural characterization.

Interrupted heat treating was utilized in an attempt to approach in-situ observation capabilities of the sequence of AGG. A region of the material from the axisymmetrically similar region (with regard to forging temperature, strain, and strain rate) in the Gleeble samples that created AGG conditions was used for interrupted heat treating and scanning electron microscopy – electron backscattered diffraction (SEM-EBSD) characterization. Post heat-treatment microstructures between the specimen utilized for interrupted heat treating and non-interrupted heat treating were compared and confirmed the interruption process of cooling and reheating did not influence final results. SEM-EBSD mapping results following the same spatial region are shown in **Figure 34.3** for conditions of (a) as forged at 1120°C to 0.15 strain and 1E-3 strain, followed by heat treating to temperatures of (b) 1130°C, (c) 1150°C, and (d) 1170°C at a heating rate of 0.13°C/s; note the grain coloring changes in **Figure 34.3c** due to specimen rotation issues. Interestingly, significant AGG occurs below the  $\gamma'$  solvus temperature, indicating the remaining  $\gamma_1'$  provides insufficient Zener pinning force to prevent AGG of  $\gamma$ . As expected, the  $\gamma$  growth continues until the abnormally large grains impinge upon each other, with remaining  $\gamma$  grains being consumed at higher temperatures. Interestingly, the grain boundary of the abnormally large  $\gamma$  appears capable of passing around existing  $\gamma$  grains and fully encapsulating them, as observed in **Figure 34.3**. Multiple instances of this have been observed in various specimens undergoing AGG, and it is believed to not be just an instance of sectioning effects. A possible explanation for this corroborates with the HERX mechanism, involving recrystallization of a  $\gamma$  grain off a  $\gamma_1'$  precipitate (with the  $\gamma_1'$  existing incoherently at a grain boundary site between neighboring  $\gamma$  grains) and growth of the HERX  $\gamma$  grain to encapsulate the existing unrecrystallized  $\gamma$  grain.

If AGG does indeed occur as a result of the theorized HERX mechanism, as these initial findings suggest, the  $\gamma_1'$  phase fraction, size, and distribution are of importance. While the secondary  $\gamma'$  are likely dissolved at isothermal forging and heat treating temperatures, the  $\gamma_1'$  exists and serves as AGG nuclei location sites. Heat treating at sub- and super-solvus temperatures for various time (2 minutes, 5 minutes, and 30 minutes) have been performed. Various etching, electropolishing, imaging techniques, and image processing methods are being evaluated and tested for determining  $\gamma_1'$  fraction.

### 34.4 Plans for Next Reporting Period

On going work is focused on refining the temperature resolution of the interrupted heat treated specimen testing to better track the progression of AGG and interaction with neighboring grains. Temperature ranges will focus on the sub-solvus regimes to include  $\gamma_1'$ . In addition to SEM-EBSD, SEM-EDS (electron dispersive spectroscopy) may assist in detecting  $\gamma_1'$  coherent with the  $\gamma'$  matrix (resolvable via local depletions of chromium) exist for HERX nuclei. Determining the conditions for HERX, whether dynamic recrystallization or static recrystallization with a possible incubation time, will also be evaluated during these interrupted heat treating specimens. Ideally, these experiments will capture and track the AGG nuclei growth. These interrupted 2-D experiments are precursors to develop (and evaluate existing) mechanistic theories and experimental procedures for in-situ 3-D and diffraction experiments.

Fraction, size, and distribution of remaining  $\gamma_1'$  in undeformed specimens will be explored. Additionally, the specimens deformed at various strain rates will be evaluated as well to determine effect of high temperature strain on  $\gamma_1'$  stability.

### 34.5 References

- [34.1] M.C. Hardy, B. Zirbel, G. Shen, R. Shankar. Developing damage tolerance and creep resistance in a high strength nickel alloy for disc applications, *Superalloys* (2004) 83-90.
- [34.2] E. Raymond, E. Huron, S. Srivasta. Control of grain size via forging strain rate limits for R'88DT, *Superalloys* 49 (2000) 49-58.
- [34.3] I.M.D. Parr, T.J. Jackson, M.C. Hardy, D.J. Child, C. Argyrakis, K. Severs, V. Saraf, J.M. Stumpf. Inhomogeneous grain coarsening behavior in supersolvus heat treated nickel-based superalloys RR1000, *Superalloys* (2016) 447-456.
- [34.4] E.J. Payton, Characterization and modeling of grain coarsening in powder metallurgical nickel-based superalloys, The Ohio State University, 2009.
- [34.5] M.A. Charpagne, J.M. Franchet, N. Bozzolo. Overgrown grains appearing during sub-solvus heat treatment in a polycrystalline  $\gamma$ - $\gamma'$  Nickel-based superalloy, *Materials and Design* 144 (2018) 353-360.
- [34.6] W. Tu, T.M. Pollock. Grain scale straining processes during high temperature compression of a PM disk alloy, *Superalloys* (2008) 395-403.

### 34.6 Figures and Tables

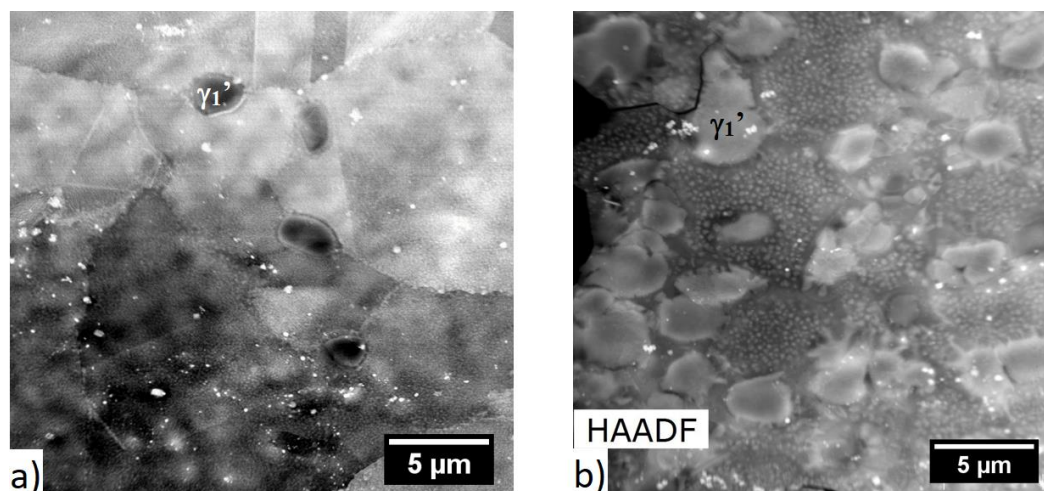


Figure 34.1: TEM micrographs of starting material conditions for 'Slice' 1 (a) and 2 (b). Slice 1 has primary  $\gamma'$  shown in darker regions, with secondary  $\gamma'$  dispersed throughout the  $\gamma$  grains. Slice 2 shows higher volume fraction of primary  $\gamma'$  and larger secondary  $\gamma'$ . Note the white speckles is a sample contamination artifact. Courtesy of Y. Guo, Mines.



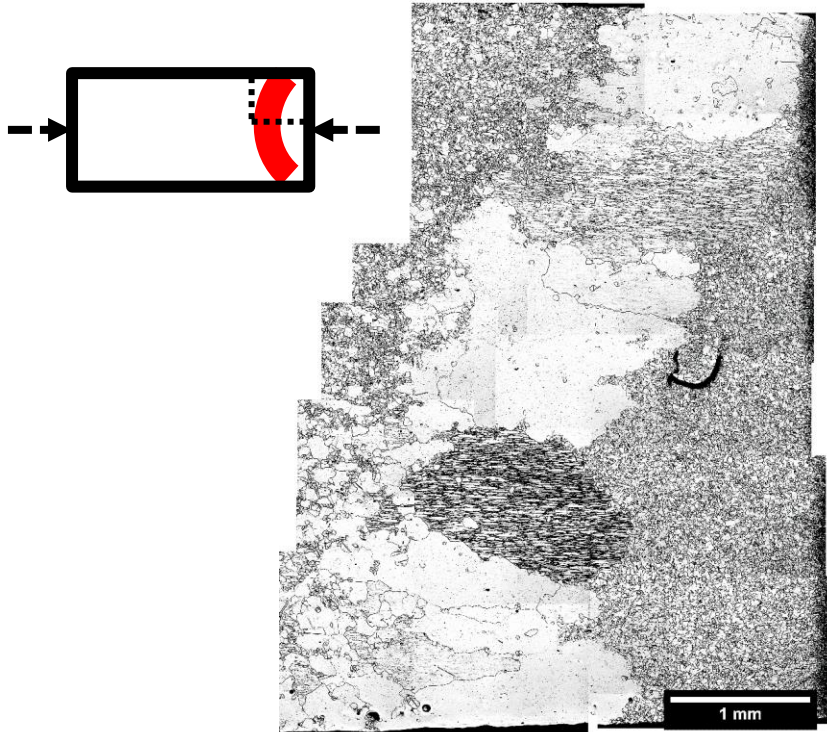


Figure 34.2: Micrograph of abnormal grain growth near the corner of an isothermal compression specimen. Note the band of abnormal grains following a specific strain and strain rate region. Schematic with dashed box showing location of micrograph on isothermal compression specimen.

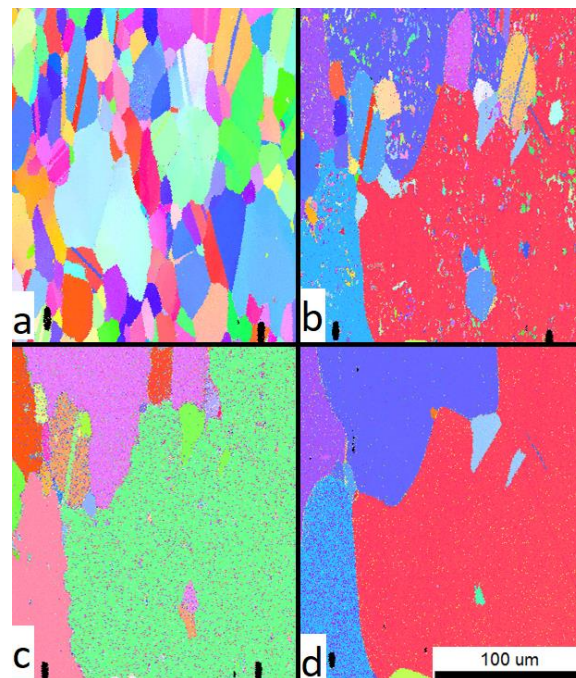


Figure 34.3: SEM-EBSD map of a constant region progressing through abnormal grain growth. Micrographs illustrate (a) as-forged microstructure (b) heated to 1130°C (c) 1150°C (d) 1170°C. Note that the  $\gamma'$  solvus temperature is nominally 1135°C. Additionally, SEM-EBSD image quality was reduced due to insufficient removal of surface oxidation with mechanical polishing techniques, as particularly seen in artifacts of micrograph (b).